Primary Transmitter Discovery based on Image Processing in Cognitive Radio

Liliana Bolea, Jordi Pérez-Romero, Ramón Agustí, Oriol Sallent

Universitat Politècnica de Catalunya (UPC)
c/ Jordi Girona, 1-3, 08034,Barcelona, Spain
{lilianab, jorperez, ramon, sallent}@tsc.upc.edu

Abstract. The subject of secondary spectrum usage has been a hot research topic for some time now. Secondary users should be able to detect available primary frequency bands and use these spectrum opportunities without causing any harmful interference to primary users. The aim of this paper is to propose a new methodology, based on image processing techniques, which combines a number of sensed samples at different random geographical positions collected by secondary sensors, in order to build a map with the positions and coverage areas of the different primary transmitters. The results can be used to discover frequencies that can be used by a secondary market without causing interference to primary receivers and without any type of cooperation between primary and secondary networks.

Keywords: Sensing, Secondary Spectrum Use, Radio Environment Map, Image Processing.

1 Introduction

Recent years have witnessed the evolution of a large plethora of wireless technologies with different characteristics, as a response of the operators' and users' needs in terms of an efficient and ubiquitous delivery of advanced multimedia services. As a result, current and future wireless scenarios will be characterized by a multiplicity of Radio Access Technologies (RATs) and network operators with very different deployments (e.g. cellular, wireless local area networks, etc.). In addition to this, and with the objective of ensuring an efficient utilization of the available spectrum bands, the regulatory perspective on how the spectrum should be allocated and utilized is evolving as well [1]. New technical advances are focused on the development of strategies and policies aiming at the utmost and efficient access to shared spectrum resources. As an example, the unlicensed use of VHF and UHF TV bands by secondary users, provided no harmful interference is caused to the licensee (i.e. primary user), was targeted by the FCC in [2].

The primary-secondary spectrum sharing can take the form of cooperation or coexistence. Cooperation means there is explicit communication and coordination between primary and secondary systems, and coexistence means there is none. In the latter case, secondary devices are essentially invisible to the primary and all of the

complexity of sharing is borne by the secondary without changes required to the primary system. In this context, one of the key enabling technologies to enable secondary spectrum access is the cognitive radio, which allows the terminals determining which portions of the spectrum are available, selecting the most appropriate channel for transmission, and vacating the channel whenever a licensed user is detected [3].

In the above framework, assuming the coexistence case, knowledge about the primary transmitters' positions can be a relevant input for secondary users to determine the frequencies available for secondary use at the different points. In this respect, this paper proposes a new methodology, based on image processing techniques, aimed at combining a number of sensed samples at different geographical positions collected by secondary sensors, in order to build a map with the estimated positions and coverage areas of the different primary transmitters. The proposed methodology could be used to build databases containing the relevant aspects of radio environment characterization, such as the so-called Radio Environment Map (REM) in [4]. The REM can serve as the navigator and the vehicle of network support for Cognitive Radios. REM can also be viewed as the generalization of the available resource map proposed by Krenik for cognitive radio applications in unlicensed wide area networks [5], [6]. In [4], the authors use the REM as a database in order to compute the distance between the primary transmitter and secondary receiver. Prior work of the authors in [7] also introduced the image processing to identify the homogeneous radio-electrical regions where certain frequencies can be detected. This paper goes beyond the previous work in [7] by introducing novel object-based reconstruction techniques to enable the characterization of the scenario based on only a subset of samples.

This paper is organized as follows. Section 2 presents the problem formulation and the scenario considerations, prior to describing the proposed methodology in Section 3. Illustrative results are presented in Section 4 and conclusions are summarized in Section 5.

2 Scenario considerations and problem formulation

A generic scenario such as the one depicted in Fig. 1 is considered. It is characterized by a number of primary transmitters corresponding to different RATs which operate at different frequencies and have different coverage areas (e.g. the central transmitter operating in a broadcast-like RAT with an extensive coverage area at frequency f_5, or the transmitters operating at RATs 1 and 2 with frequencies f_1, f_2, f_3 and f_4 that could correspond to some cellular-like RATs). Assuming that no cooperation between the primary and secondary networks exists, the secondary network will have to discover the positions and coverage areas of the primary transmitters to be able to decide in which places and in which frequencies secondary transmissions could be allowed. For that purpose, the secondary network can rely on the information measured by a number of sensors randomly scattered in the scenario and that could be built-in e.g. mobile terminals, and the appropriate post-processing of this information, which is the focus of this paper.

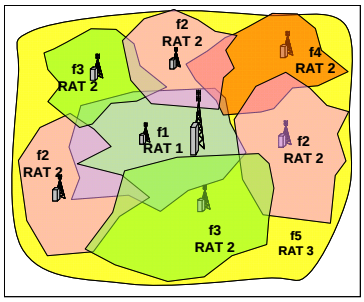

Fig. 1 Generic scenario with different RATs and frequencies

A sensor measures the received power in a number of specific frequencies in its position. It is assumed that frequency f_i is detected by the sensor at position (x,y) when the received power is above a given threshold $P_{th}(f_i)$, so that the following binary representation can be obtained for each frequency at each sensor position:

$$M(f_i,x,y)=\begin{cases}1 & \text{if } f_i \text{ detected in}(x,y)\Leftrightarrow \text{if } P(f_i,x,y)\geq P_{th}(f_i)\\ 0 & \text{if } f_i \text{ not detected in}(x,y)\Leftrightarrow \text{if } P(f_i,x,y)< P_{th}(f_i)\end{cases} \quad (1)$$

From this binary representation, it is possible to characterize the measurement at all frequencies given by the sensor at coordinate (x,y) by a value corresponding to the sum of the binary representations of all the N considered frequencies:

$$I(x,y)=\sum_{i=1}^{N} M(f_i,x,y)\,2^{i-1} \quad (2)$$

Each sensor would then report the value of $I(x,y)$ to a central entity in charge of combining the measurements of every sensor. The problem considered here consists then in defining a methodology to smartly combine the different measurements at random positions, which represent a partial vision of the scenario, in order to get a full vision in which the positions and coverage areas of the different primary transmitters are obtained. It is worth mentioning that this work focuses mainly on this combination of the sensing results, assuming these results are available, but both the considerations on the sensing process itself (such as errors in the process or the determination on which frequencies has to sense every sensor) and the means to report the sensing results are out of the scope of the paper and are left for future work.

3 Proposed methodology

The proposed methodology assumes that the radio environment can be characterized by an image [7], where each pixel (i.e. a rectangular area of dimensions $\Delta x \times \Delta y$) takes the value $I(x,y)$ corresponding to the frequencies that are detected in it. Then, given that only the values $I(x,y)$ of the pixels where a sensor is located are known, these values need to be combined using image processing techniques in order to

reconstruct the overall image and to discover the transmitter positions and coverage areas, as it is illustrated in Fig. 2. It is assumed that a pixel can only have the result of one sensor.

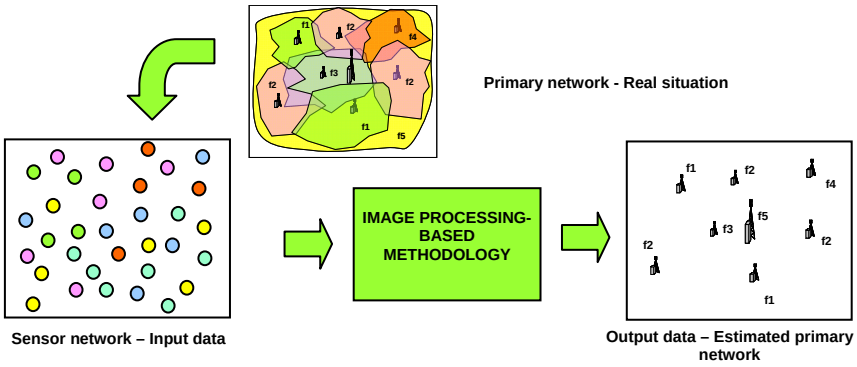

Fig. 2 Inputs and outputs of the considered problem

Assuming that the coverage area of a transmitter to be discovered will be approximately circular, which would be valid according to the distance-dependent path loss whenever omnidirectional antennas are used, the proposed methodology aims at identifying in the image the existing circular regions. For that purpose, starting from the sensed pixel values, which will be affected by propagation and shadowing effects, an object-based reconstruction technique will be developed to identify those "objects" (i.e. an object is a region where a certain frequency f_i is detected) that can be assimilated as circular areas and correspondingly as transmitter coverage areas. For that purpose, the steps of the proposed methodology are illustrated in Fig. 3 and explained in the following.

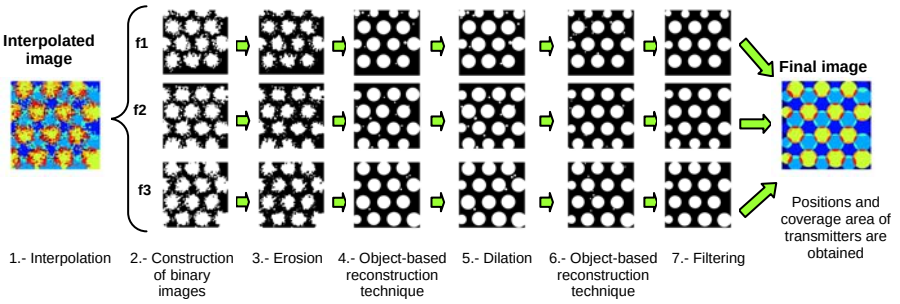

Fig. 3 Steps of the proposed methodology

3.1 Interpolation

Interpolation is the first step of this methodology. From the results of the sensors we build an image by interpolating the intermediate pixels for those positions where no sensor was available. We do that by attributing to each unknown pixel the value of the nearest known pixel.

3.2 Construction of binary images

From the interpolated image, we build a set of binary images, each one corresponding to a given frequency f_i. Each pixel of a binary image takes the value 1 if frequency f_i is detected and 0 otherwise. These binary images will be used as the basis to identify the different objects.

3.3 Erosion

It is possible that in some cases, some objects are not properly detected in the binary images, because they are not clearly separated from each other. This can occur due to e.g. shadowing effects in the propagation. In order to eliminate this drawback, before the object-based reconstruction technique, we apply an image processing technique called *erosion* to the binary images resulting from the interpolated image. In the erosion, the value of the output pixel is the minimum value of all the pixels in the input pixel's neighborhood. We assume that a pixel's neighborhood is defined by a circular area of radius 5 pixels. In image processing terminology, this corresponds to making the erosion with a circular structuring element [8]. Note that in the particular case of a binary image, if any of the pixels of the neighborhood is set to the value 0, the output pixel after the erosion will be set to 0, which will tend to decrease the size of the objects and thus to separate them.

3.4 Object-based reconstruction technique

Object-based reconstruction technique tries to regenerate the image based on object properties, in particular assuming that the coverage area of a transmitter will be approximately circular. For each binary image (i.e. for each frequency f_i), we:

- Detect the objects (i.e. regions where frequency f_i is detected), following the so-called *connected-component labelling* technique [9] that consists in scanning the image and making groups of adjacent pixels having the same value (4-connected pixels are assumed, meaning that pixels are adjacent if their edges touch). Each group of pixels will be then an "object".
- Measure objects properties (centroid and diameter of the object, which correspond to the centre and diameter of a circle with equivalent area than the object). Note that the centroid of every object represents the estimate position of primary transmitter;
- Regenerate a new image replacing each object by a circle with the corresponding diameter (see Fig. 3).

3.5 Dilation

Because of the prior erosion process, the resulting object area after object-based reconstruction technique has become smaller than in the binary images, which would lead to more reduced coverage areas than in the real situation. To compensate this

effect, we apply the *dilation* technique to the binary images resulting from the object-based reconstruction technique. The dilation is the image processing technique opposite to the erosion process, and in this case the value of the output pixel is the maximum value of all the pixels in the input pixel's neighborhood [8]. In particular, in a binary image, if any of the pixels of the neighborhood is set to the value 1, the output pixel is set to 1, which will tend to increase the size of the objects. The same neighborhood shape (i.e. circular structuring element) as in the erosion is considered.

3.6 Object-based reconstruction technique

After the dilation process, it may occur that some small circles intersect with other bigger circles. For that purpose, we execute again the *object-based reconstruction technique* to clearly regenerate the circular areas.

3.7 Filtering

Due to the shadowing effects in the propagation, after the reconstruction process, it may happen that certain objects are detected with an area significantly smaller than that of the rest of objects, so they cannot be considered as transmitters. To cope with this, in the last step, we *filter* the resulting images by eliminating those objects that have an area 30 times smaller than the average area of all the detected objects.
Finally, after the filtering, we combine the binary images to obtain a new image including information of all the frequencies. This image includes the positions, coverage areas and frequencies of the different primary transmitters.

4 Results

In order to illustrate the capabilities of the proposed methodology, it is evaluated in a cellular scenario with cell radius 1km, hexagonal layout and with a 3 frequency reuse pattern (f_1, f_2, f_3). The total scenario size is 10km x 10km, and the pixel size is $\Delta x=\Delta y=10$m. The transmitter power is 30dBm, propagation losses as a function of distance d(km) are given by $L=128.1+37.6*\log_{10}(d)$ and the shadowing standard deviation is 3dB. Power threshold $P_{th}(f_i)$ is set at -99.6dBm for all frequencies. In Fig. 4 we can see the original image corresponding to the digitalization (i.e. the image if all the pixels were known). Having just N=3 frequencies, pixels are encoded according to equation (2) with $8=2^N$ different intensity levels (i.e. colours) where the value 7=111 corresponds to the areas where three cells are overlapped, the values 3=011, 5=101 and 6=110 corresponds to the areas where two cells overlap and finally the values 1=001, 2=010 and 4=100 correspond to the central areas of each cell.

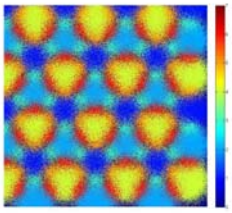

Fig. 4 Image corresponding to the cellular scenario with 3dB standard deviation shadowing. In the right part, the colour scale corresponding to each pixel intensity between 0 and 7 is plot

We sense the original image with a random sensor distribution with average density D sensors/km^2 and apply the proposed methodology. In Fig. 5 we can see the difference between the original image with shadowing effects, the sensed and interpolated image and the reconstructed image, in case that density of sensors D=100sensors/km^2. Visually we can remark that we obtain an important improvement of the original image as the shadowing effects are no longer included in the reconstructed image, so that the positions and coverage areas of the different transmitters can be more clearly identified.

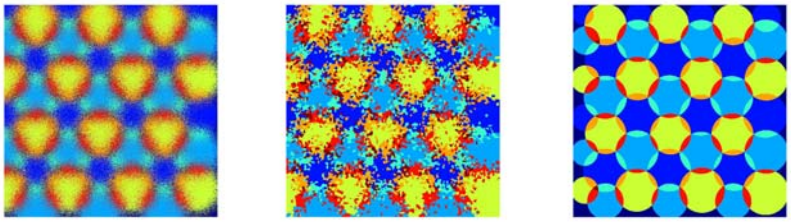

Fig. 5 Comparison between the original image, the sensed and interpolated image, and the reconstructed image for the case D=100 sensors/km^2

In Fig. 6, we observe the resulting images for different values of the sensor density D. Note that if we have a low density of sensors such as D=4sensors/km^2, we can not properly identify the transmitters.

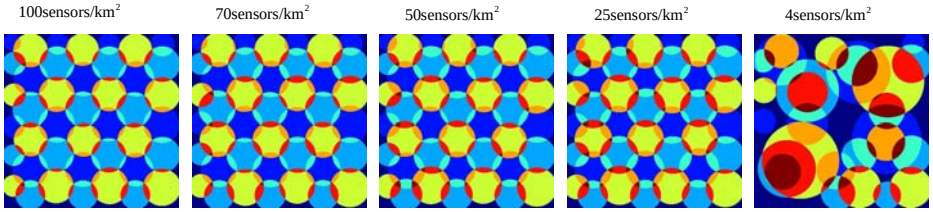

Fig. 6 Images resulted after proposed methodology for different sensor densities

Every centroid of the detected objects represents the estimation of the position of each transmitter. In order to measure the accuracy in this estimation, we compute the

relative error in the position estimation as the difference between the real transmitter position and the detected position, divided by the transmitter coverage radius. For this computation, we do not account for the transmitters that are located in the borders of the image, since they do not form a complete circle in the original image and consequently they lead to larger errors due to border effects.

Fig. 7 represents the relative error for each transmitter in the considered scenario in case that density of sensors D=100sensors/km^2. It can be observed that, in all the cases, the values of the relative errors are below 8%.

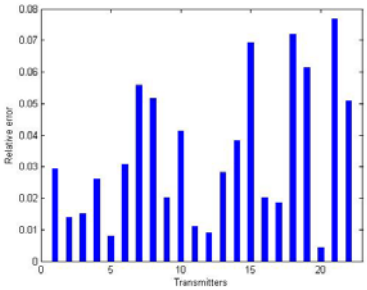

Fig. 7 Relative error in the transmitter positions for D=100sensors/km^2

The mean error and the standard deviation for different density of sensors are shown in Fig. 8. In addition, Fig. 9 plots the rate of transmitter detection representing the ratio between the number of transmitters properly detected and the exact number of transmitters. In case that density of sensors D=4 sensors/km^2, only a 40% of the transmitters are detected, and the mean error is high, as well as the standard deviation. As the density of sensors grows, the rate of detection is 100%, and the mean error is smaller. Gathering more than about 25 sensors per km^2 (i.e. on average 1 sensor every 200×200 m^2 or equivalently about 80 sensors per transmitter coverage area) leads to minor marginal gains to the mean error of about 5% (or 50 meters in the base station position) and to a detection probability of 100% in the analysis performed.

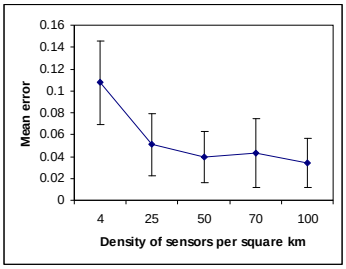

Fig. 8 Mean error and standard deviation, represented as vertical lines.

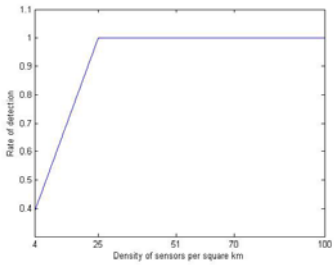

Fig. 9 Rate of transmitter detection

Fig. 10 and Fig. 11 plot the obtained results for different values of cell radius. As we expect, in case that the cell radius is small (e.g. 500m), we have fewer sensors inside the cell coverage area, the errors are bigger, and the rate of detection smaller. Instead, if the cell radius is large (e.g. 1500m), the number of sensors inside the cell coverage area is also larger, the errors are smaller and the rate of detection is higher.

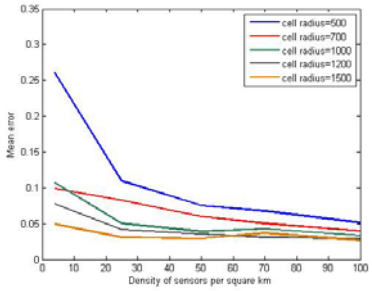

Fig. 10 Mean error for different values of cell radius.

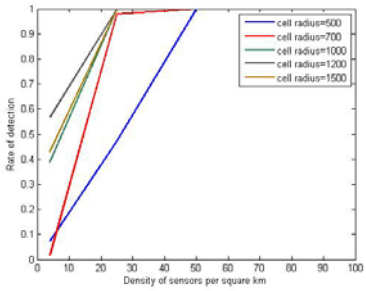

Fig. 11 Rate of transmitter detection for different values of cell radius

Accepting an error below 5% and a rate of transmitter detection above 95%, we can obtain from the results the minimum density of sensors necessary in order to make a proper estimation of the position of the transmitters. This is indicated in Table 1.

Table 1 Minimum density of sensors necessary for different cell radius

	cell radius 500 m	cell radius 700 m	cell radius 1000 m	cell radius 1200 m	cell radius 1500 m
density of sensors per km^2	110	73	28	22	10

5 Conclusions

This paper has presented a new methodology, based on image processing techniques that combine a number of sensed samples at different geographical positions collected by sensors, in order to discover the positions and coverage areas of the different primary transmitters. Utilization of these databases in a secondary spectrum usage permits the secondary network to discover the presence of primary network transmitters and to use spectrum opportunities without disturbing the primaries. The results obtained reveal the utility and efficacy of the proposed methodology, with relative errors below 5% in the transmitter position.

Acknowledgments. This work has been supported by the Spanish Research Council and FEDER funds under COGNOS grant (ref. TEC 2007-60985).

References

1. Cave, M.: Essentials of modern spectrum management, Cambridge University Press, (2007).
2. Federal Communications Commission (FCC): Notice of Proposed Rule Making, ET Docket no. 04-113, May 25, (2004).

3. Akyildiz, I.F., Lee W.-Y., Vuran M.C., Mohanty S.: Next generation/dynamic spectrum access/cognitive radio wireless networks: a survey, Computer Networks, Vol. 50, No. 13, pp. 2127–2159, (2006).
4. Zhao. Y., Raymond, D., da Silva, C. R. C. M., Reed, J. H., Midkiff, S. F.: Performance evaluation of radio environment map-enabled cognitive spectrum-sharing networks, in Proc. IEEE Military Comm. Conf., Orlando, FL, pp. 1--7, (2007).
5. Krenik W, Batra A, - Cognitive Radio Techniques for Wide Area Networks, Proc. Conference on Design Automation, pp. 409-412, 2005.
6. Krenik W,. Panasik C, - The Potential for Unlicensed Wide Area Networks, Wireless Advanced Architectures Group, Texas Instruments White Paper, November 2004;
7. Pérez-Romero, J., Sallent, O., Agustí, R.: On the Applicability of Image Processing Techniques in the Radio Environment Characterisation, 69th IEEE Vehicular Technology Conference: VTC 2009 Spring, Barcelona, Spain, (2009).
8. "Morphological operations", Image Processing Toolbox, The Mathworks. Available at: http://www.mathworks.com/access/helpdesk/help/toolbox/ images/index.html.
9. R. Fisher, S. Perkins, A. Walker and E. Wolfart (2003): Connected Component Labeling. Available at: http://homepages.inf.ed.ac.uk/rbf/HIPR2/label.htm#1.